Pharmacologic Induction of Heme Oxygenase-1 Plays a Protective Role in Diabetic Retinopathy in Rats

Jiawen Fan,[1] *Gezhi Xu,*[1,2] *Tingting Jiang,*[1] *and Yaowu Qin*[1]

Purpose. We investigated the protective effects of HO-1, induced by hemin, in the retinas of streptozotocin (STZ)-induced diabetic rats, and document the possible anti-inflammatory, anti-apoptotic, and anti-proliferative mechanisms underlying the protection.

Methods. Sprague-Dawley (SD) rats were induced to diabetes by intraperitoneal injection of STZ (60 mg/kg). Later, some of the rats were given intraperitoneal injections of hemin (20 mg/kg) to induce expression of HO-1. The protective effects of hemin were evaluated by examining the hemoglobin concentration (Hb) and the glycosylated hemoglobin (HbA1c) level of blood from the rats, further calculating the numbers of TUNEL positive cells in retinal ganglion cell (RGC) layer and dil-labeled RGCs. We also documented the expressions of HO-1, HIF-1α, SOD-1, VEGF, p53, and bcl-2 by Western blot analysis and real-time quantitative PCR. Expressions of Nrf2, tERK 1/2;, and pERK 1/2 were detected only by Western blot analysis. HO-1, Nrf2, pERK, and GFAP proteins were detected by immunofluorescence.

Results. The Hb level was higher in hemin-treated rat blood than nontreated diabetic group, while the HbA1c level was lower. Hemin significantly activated HO-1 expression in the retinas of diabetic rats, combined with accordant changes of Nrf2/pERK protein expression, and upregulated the expression of GFAP in retina. Retinal ganglion cells displayed greater sensitivity to apoptosis when the HO-1 level was lower. Overexpression of HO-1 was associated with an increase in the activation of SOD-1 and bcl-2, and a decrease of the expression of HIF-1α, VEGF, and p53.

Conclusions. HO-1 is an important positive modulator of the Nrf2/ERK-related signaling. Overexpression of HO-1 by hemin induction protected retinal ganglion cells in diabetic retinopathy through anti-inflammatory, anti-apoptotic, and anti-proliferative effects. (*Invest Ophthalmol Vis Sci.* 2012;53:6541–6556) DOI:10.1167/iovs.11-9241

Diabetic retinopathy (DR) is a progressive neurodegenerative disease that results in the cellular dysfunction of multiple types of cells in the retina. In response to the diabetic microenvironment, all types of retinal cells undergo a series of changes in function and structure, including apoptosis of retinal ganglion cells (RGCs) and metabolism of Müller glial cells.[1,2] Despite having identified multiple pathogenic mechanisms in DR, the treatment methods of this disease are limited. Since DR was described as diabetic retinitis, inflammatory processes in the retina, including oxidative damage, neuron apoptosis, and cell proliferation, have attracted increasing attention.

Heme oxygenase (HO), a stress-responsive enzyme, also is the rate-limiting enzyme in heme catabolism. HO degrades free heme to yield equimolar amounts of gas carbon monoxide (CO), iron, and biliverdin. Iron induces the expression of heavy-chain (H-) ferritin (H-ferritin), and biliverdin is converted to bilirubin by biliverdin reductase. The function of HO-1 is to prevent the accumulation of highly deleterious free heme.[3] The byproducts (CO, biliverdin, bilirubin, and H-ferritin) produced in the process of heme-HO reaction all are antioxidants, anti-inflammatories, and modulators of cell death and proliferation.[4,5] These byproducts can promote the return to homeostasis after the onset of many pathologic conditions by different mechanisms. Two distinct mammalian HO isoforms have been identified and characterized: HO-1 and HO-2. HO-1, an inducible protein, is expressed ubiquitously and is induced strongly by numerous stress stimuli in diabetes, including heat shock, oxidative injury, and microvascular and macrovascular complications.[6–9] In the retinas of rats, HO-1 is overexpressed in response to ischemia-reperfusion injury.[10,11] Induction of HO-1 could be a part of the retina's anti-apoptosis system of defense against light-induced damage to the photoreceptors in rats.[12] HO-1 also can be induced by heavy metals and their substrate, hemin (ferriprotoporphyrin IX).[13,14] Hemin induces the upregulation of HO-1 gene expression, and prevents an inflammatory response in vascular endothelial cells and glial cells, lung injury, and liver damage.[15–18] Nonetheless, the underlying mechanisms remain largely unknown.

The induction of the HO-1 gene is primarily regulated at the transcriptional level; the pharmacological abilities of hemin and polyphenols to induce HO-1 is linked to the transcription factor nuclear factor-erythroid 2 (NF-E2)-related factor 2 (Nrf2).[18,19] Nrf2 recently has attracted considerable interest from researchers investigating inflammatory disorders and neurodegenerative diseases.[20,21] The extracellular signal-regulated kinase (ERK) signaling pathway of mitogen-activated protein kinase (MAPK) family appears to be involved to some extent in HO-1 expression and Nrf2 nuclear translocation in response to diverse stimuli.[18,22,23] In the retinas of diabetic subjects, the ERK1/2 signaling pathway has a key role in high glucose-induced stress and VEGF release.[24,25]

We investigated the induction of HO-1 in the rat retina by hemin. We hypothesized that Nrf2 and ERK1/2 signaling activation is related to the overexpression of HO-1. Furthermore, to determine a potential target for treatment, we investigated the effect of hemin treatment, and illuminated the underlying anti-inflammatory, antioxidant, anti-apoptotic,

From the [1]EENT Hospital, Eye Institute, Fudan University, Shanghai, China; and [2]Institute of Brain Science, Fudan University, Shanghai, China.

Supported by National Basic Research Grants of China (30872825, 2008 and 81170857, 2011) and by Program of Shanghai Subject Chief Scientist (A type, 09XD1400900).

Submitted for publication December 5, 2011; revised April 21 and May 24, 2012; accepted May 24, 2012.

Disclosure: **J. Fan**, None; **G. Xu**, None; **T. Jiang**, None; **Y. Qin**, None

Corresponding author: Gezhi Xu; xugezhi001@163.com.

and anti-proliferative mechanisms provided by hemin-induced HO-1 expression in STZ-induced diabetic rats' retina.

Materials and Methods

Experimental Animals and Intraperitoneal Hemin Treatment

Male Sprague-Dawley (SD) rats, 9 weeks of age (250 ± 20 g), were assigned at random to become diabetic or remain nondiabetic controls. Treatment of the animals conformed to the National Institute of Health Principles of Laboratory Animal Care and the ARVO Statement of the Use of Animals in Ophthalmic and Vision Research, and local institutional guidelines. Diabetes was induced by a single intraperitoneal injection of streptozotocin (60 mg/kg body weight; Sigma, Poole, UK) in SD rats (9 weeks of age). Age-matched control rats were injected with citrate buffer (6.0 mL/kg) using the same method. Animals with plasma glucose levels greater than 16.0 mmol/L 3 days after streptozotocin injection were considered diabetic. Plasma glucose level and weight of animals were monitored once a week for the 3 months of the study and just before the rats were euthanatized by an overdose of pentobarbital at 2, 4, 6, 8, or 12 weeks after the onset of diabetes. The same methods were used for the age-matched normal control group.

For the preparation of injection, hemin (Sigma) was dissolved first in 0.2 M NaOH, adjusted to a pH of 7.4, and diluted to a final concentration of 0.01 M with physiologic saline. The hemin solution must be used within 1 hour after preparation. Rats that were induced with diabetes by streptozotocin were given intraperitoneal injections of hemin (20 mg/kg body weight as therapy group) on alternate days from the onset of diabetes until euthanatized at 4 or 8 weeks. The normal rats were given intraperitoneal injections of physiologic saline (3 mL/kg body weight as vehicle group) on alternate days, lasting 8 weeks. Compared to the hemin(+) therapy group, the hemin(–) nontreated diabetic rats were the blank group. The experimental groups and numbers of animals at each time point of each group are presented in Table 1. In each group, one eye of each rat was removed and made into paraffin-embedded sections or frozen sections for TUNEL labeling and immunofluorescence. The retina of the other eye was isolated and frozen immediately in liquid nitrogen for biochemical measurements (Western blots and real-time PCR).

Table 1. Number of Experimental Animals at Each Time Point in Each Group

	Nondiabetic Control Rats		Diabetic Rats (DM)	
	Normal Group*	Vehicle Group	Blank Group	Therapy Group
2 wk	18	–	18	–
4 wk	18	–	18	18
6 wk	18	–	18	–
8 wk	18	18	18	18
12 wk	18	–	18	–

* If there was no significant difference at all the five time points of the normal group, results just showed a random age-matched control group as the normal group.

Blood Collection and Hematological Examination

Whole blood samples were collected from the femoral vein into evacuated tubes containing EDTA solution as anticoagulant. The tube was conserved at 4°C (within 24 hours after collection) and used for determination of hematological parameters. Red blood cells count (RBC) and hemoglobin concentration (Hb) were measured by blood cell analyzer CELL-DYN 3700 (Abbott Laboratories, Abbott Park, IL). Glycosylated hemoglobin (HbA1c) were measured by automatic glycosylated hemoglobin analyzer AC6000 (Audicom Medical Technology Co., Ltd., Jiangsu, China).

Real-Time Quantitative PCR

Quantitative real-time PCR was performed using a thermal cycler (Stepone Plus; Applied Biosystems, Carlsbad, CA). The $2^{-\Delta\Delta C}{}_T$ analysis method was used to quantify relative amounts of mRNA.[26] For normalization of gene expression levels, mRNA ratios relative to the house-keeping gene β-actin were calculated. Total RNA was isolated from the retina using an extraction reagent (TRIzol; Invitrogen, Carlsbad, CA) and 1 μg total RNA was reverse-transcribed with 1 μM oligo(dT) and Superscript reverse transcriptase (Promega, Shanghai, China). cDNA was amplified in a 20 μL reaction containing 1 μL of cDNA template, 10 μL of iSYBR supermix (Biotnt, Shanghai, China), 0.2 μM each of upstream- and downstream-primer, and double-distilled H_2O. Exon-spanning primers (synthesized by Invitrogen, Shanghai, China), designed by means of Primer 5.0 software (Premier Biosoft International, Palo Alto, CA), and PCR conditions are summarized in Table 2. After an initial denaturation step of 95°C for 5 minutes, PCR involved 40 cycles at 95°C for 5 seconds, 60°C for 30 seconds, and 72°C for 10 seconds.

Western Blot Analyses for HO-1, Nrf2, tERK, pERK, HIF-1α, SOD-1, VEGF, bcl-2, and p53

Western blot analyses of HO-1 (Abcam, Hong Kong, China), Nrf2 (Abcam), total ERK1/2 (tERK; Cell Signaling Technology, Danvers, MA), phosphorylated ERK1/2 (pERK; Cell Signaling Technology), HIF-1α (Epitomics, Burlingame, CA), SOD-1 (Epitomics), VEGF (Abcam), bcl-2 (Chemicon, Temecula, CA), and p53 (Chemicon) were performed using the respective antibodies. The whole retina was isolated carefully and placed into 100 μL of lysis buffer (7 M urea, 32.5 mM CHAPS, 2 M thiourea, 50 mM dithiothreitol, 100 mM PMSF, [pH 7.5]) supplemented with protease inhibitors (2 mg/L aprotinin, 100 μM phenylmethylsulfonyl fluoride, 10 μM leupeptin, 2.5 μM pepstatin A) and sonicated. The lysate was centrifuged and the supernatant was collected. Each sample containing 30 μg of total protein was separated by SDS-PAGE, and electroblotted to polyvinylidene fluoride (PVDF) membranes (Milipore, Billerica, MA). After nonspecific binding was blocked with 5% BSA, the membranes were incubated with a rabbit polyclonal antibody against HO-1 (1:2000), Nrf2 (1:1000), tERK (1:1000), pERK (1:1000), HIF-1α (1:2000), VEGF (1:500), SOD-1(1:1000), bcl-2 (1:2000), and p53 (1:1000) at 4°C overnight, followed by incubation with a horseradish peroxidase (HRP)-linked goat antibody against rabbit IgG (1:2500; BioSource, Camarillo, CA). The signals were visualized with chemiluminescence (ECL kit; Thermo Scientific, Rockford, IL) according to the manufacturer's protocol.

Immunofluorescence and Confocal Microscopy

Frozen sections were used for immunofluorescence. Eye cups were fixed for 2 hours at 4°C with 4% paraformaldehyde in 0.1 M PBS, followed by immersion in a graded sucrose solution (20–30% in 0.01 M PBS) at 4°C overnight. Eye cups were embedded in optimal cutting temperature (OCT) compound (Tissue-Tek; Sakura Finetek, Torrance, CA), sectioned at 10 μm, and stored at –80°C until needed. After incubation with 0.3% Triton in 0.01 M PBS for 30 minutes at 37°C, retinal cryostat sections were incubated with a blocking solution for 30 minutes at 37°C. Immunofluorescent labeling was performed to identify immunoactive cells using primary antibodies specific for HO-1 (1:100; Abcam), Nrf2 (1:100; Abcam), pERK (1:1000; Cell Signaling Technology) and GFAP (1:500; Chemicon) at 4°C overnight. After the sections were rinsed three times with 0.01 M PBS, anti-rabbit antibodies (1:1000; Alexa Fluor 488, Alexa Fluor 555; Molecular Probes; Invitrogen, Eugene, OR) were applied as secondary antibodies and incubated at 37°C for 1 hour. Cell nuclei were counterstained with 4′-6-diamidino-2-phenylindole (DAPI; Sigma, St. Louis, MO). Images

Table 2. Primers Used for Quantitative Real-Time PCR

Gene	Accession No.	Product	Sequence
HO-1	NM_012580.2	107 bp	5′-ACCCCACCAAGTTCAAA CAG-3′ 5′-GAGCAGGAAGGCGGTCTTAG-3′
VEGFa	NM_031836.2	151 bp	5′-CAGCGACAAGGCAGACTATT-3′ 5′-GTTGGCACGATTTAAGAGGG-3′
HIF-1α	NM_024359.1	149 bp	5′-GCGAAGCAAAGAGTCTGAAG-3′ 5′-CAAGATCACCAGCACCTAGAAG-3′
SOD-1	NM_017050.1	129 bp	5′-CCACGAGAAACAAGATGACT-3′ 5′-GACTCAGACCACATAGGGAAT-3′
bcl-2	NM_016993.1	135 bp	5′-ACTTCTCTCGTCGCTACCGT-3′ 5′-CAATCCTCCCCCAGTTCAC-3′
p53	NM_030989.3	151 bp	5′-GGGAGTGCAAAGAGAGCAC-3′ 5′-CCTTTAATTCCAAGGCCTCA-3′
β-actin	NM_031144.2	231 bp	5′-AACCCTAAGGCCAACAGTGAAAAG-3′ 5′-TCATGAGGTAGTCTGTGAGGT-3′

VEGFa, vascular endothelial growth factor a; HIF-1α, hypoxia inducible factor-1α; SOD-1, Cu-Zn superoxide dismutase-1; bcl-2, B cell leukemia/lymphoma-2.

were acquired under a laser confocal microscope (FluoView FV1000; Olympus, Tokyo, Japan), using a 488-nm laser for Alexa Fluor 488 and a 543-nm laser for Alexa Fluor 555. Both fluorophores were imaged by a sequential line scan, and each image was saved at a resolution of 1024 × 1024 pixels. The optical sections were reconstructed with a maximum projection using the microscope software (OLYMPUS FV1000 Ver.1.7b Viewer, Olympus).

In Situ TUNEL Labeling

Paraffin sections were used for in situ TUNEL labeling. Eyeballs were harvested and fixed in methacarn solution (60% methanol, 30% chloroform, and 10% acetic acid) and were sectioned along the vertical meridian to include a full length of retina passing through the optic nerve head, and the superior and inferior regions of the eye. For each rat, three 4 μm thick paraffin-embedded sections that included the ora serrata and the optic nerve were stained by a TUNEL–based kit (TACS TdT Fluorescein; R&D Systems, Minneapolis, MN). The number of TUNEL-positive RGCs for each retinal section was counted in four selected retinal areas, each 0.33 mm in length. The first two segments chosen were located 0.33 mm superior and inferior to the optic nerve head, respectively, and the other two segments were 0.33 mm superior and inferior to the first two segments, respectively. The total number of TUNEL-positive RGCs of these 12 retina areas was averaged as a representative of TUNEL-positive RGCs per one eye sample.

Retrograde Labeling of RGCs

A total of 7 μL of the lipophilic tracer, 1,1′-dioctadecyl-3,3,3′,3′-tetramethylindocarbocyamine percholorate (dil; Molecular Probes, Eugene, OR) was placed on both superior colliculi for retrograde labeling of RGCs in normal group, blank group, and therapy group at weeks 3 and 7.[27] One week later, six rats were killed. Whole mounted retinas of the left eye were examined under a fluorescence microscope (DM 4000B; Leica, Wetzlar, Germany) within 3 hours of enucleation. Three selected areas (0.307 mm × 0.307 mm) at 2, 3, and 4 mm from the optic disc were photographed in the four retinal quadrants. The number of dil-labeled cells was counted in the photographs and the density of labeled RGCs/mm^2 was calculated by averaging the 12 counts in each retina.

Statistical Analysis

Data were subjected to statistical analysis by paired or unpaired *t*-tests and ANOVA (GraphPad Prism, version 5.0; GraphPad Software Inc., San Diego, CA). Newman-Keuls multiple comparison tests were used to compare the data within each experiment. Data were presented as mean ± SEM. Experiments were performed in triplicate at least. $P < 0.05$ was considered statistically significant.

Results

Glucose and Weight

After the rats had been injected with STZ, the induction of diabetes was confirmed based on the rats' blood glucose levels (>16.0 mmol/L) and weight. Of the injected rats 87.3% became diabetic. As expected, the mean blood glucose level was elevated significantly in rats from the diabetic group, compared to the age-matched control group (Fig. 1A, $P < 0.0001$, $n = 10$ at each time-point in each group). Almost all rats in the diabetic group reached the category "High 1" blood glucose level (≥33.3 mmol/L) 3 days after being injected with STZ and maintained this level until the last of the rats were euthanized at the end of 12 weeks. The mean body weight of the age-matched control rats increased gradually. Meanwhile, the mean body weight of the diabetic group decreased on the first day of confirmed diabetes, increased slightly from weeks 2 to 4, and then decreased again (Fig. 1B, $P < 0.0001$, $n = 10$ at each time-point in each group).

Effect of Hemin on Blood Hb and HbA1c of Diabetic Rats

The mean blood levels of Hb were significantly higher in the hemin-treated rats compared to the nontreated diabetic rats (Fig. 2A, $P = 0.0009$ between the therapy group and blank group at week 4, and $P = 0.0263$ at week 8; $n = 10$ blood samples at each time-point in each group). The mean blood levels of HbA1c were significantly higher in the nontreated diabetic group compared to the normal control group and a significant increase was observed from weeks 4 to 8 after administering STZ (Fig. 2B, $P < 0.0001$). The mean level of HbA1c was significantly lower in hemin-treated group, compared to the nontreated group (Fig. 2B, $P = 0.0039$ between the therapy group and blank group at week 4, and $P = 0.0051$ at week 8; $n = 10$ blood samples at each time-point in each group). The mean blood RBC level had no significant differences between treated and nontreated groups (data not shown in this study).

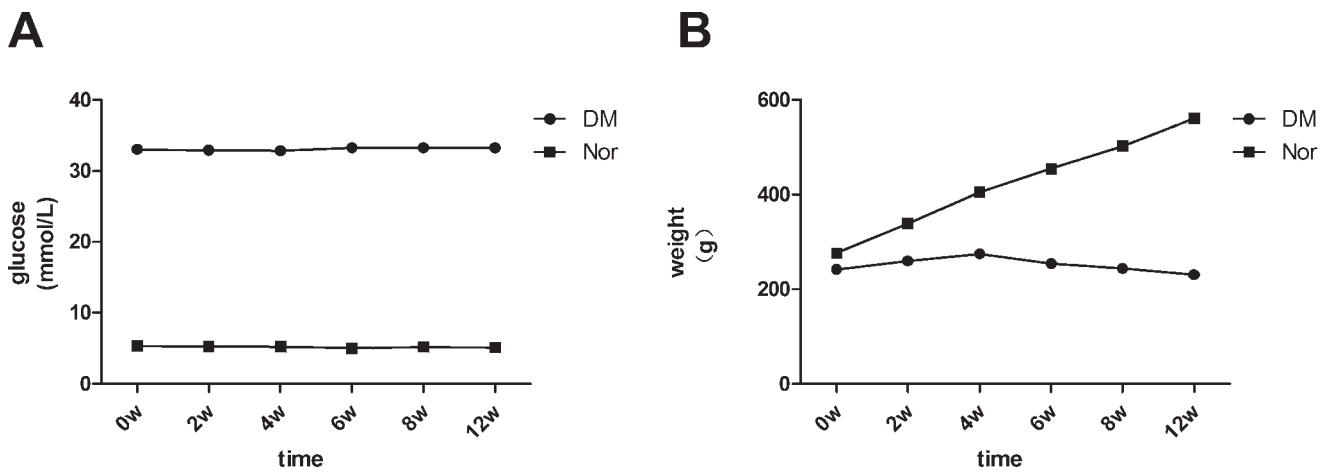

FIGURE 1. (**A**) The mean blood glucose levels were significantly higher in the diabetic group compared to the normal control group ($P < 0.001$, $n = 10$). (**B**) Mean body weight of the normal control group gradually rose, and mean body weight of the diabetic group was significantly lower than that of the normal control group in spite of slight increase at first four weeks ($P < 0.001$, $n = 10$).

Expression of HO-1 mRNA and Protein in the Retinas of Diabetic Rats

Western blot analysis of homogenized retinal tissue from diabetic rats (blank group) revealed that the expression of endogenous HO-1 was detected 2 weeks after the STZ-induced high blood glucose, peaked at week 4, and peaked a second time at week 12 (Figs. 3A, 3B). Since there were no significant differences among the five age-matched normal control groups, data just showed the 12-week-matched normal control group as the normal group (Nor). The amount of HO-1 produced at week 4 was 57.9 ± 28.89-fold greater than the amount of HO-1 produced in the normal rat retina, 4.63 ± 1.68-fold greater than week 2, and 1.94 ± 0.47-fold greater than week 6. The level of HO-1 protein in diabetic retinas was significantly higher than in normal control retinas ($P = 0.0034$, $P = 0.0003$, $P < 0.0001$, $P = 0.0009$, and $P = 0.0006$ at weeks 2, 4, 6, 8, and 12, respectively; $n = 6$ eye samples at each time-point in each group, or $n = 6$ for short in the following paragraphs). The data also showed that the amount of HO-1 protein decreased at week 6, compared to week 4 ($P = 0.012$).

Consistent with the protein data, our analysis revealed significantly higher levels of HO-1 mRNA in retinas from diabetic rats after 4 weeks, compared to the retinas of the normal controls ($P = 0.1932$, $P = 0.0127$, $P = 0.0167$, $P = 0.0256$, and $P = 0.0353$ at weeks 2, 4, 6, 8, and 12, respectively; $n = 6$; Fig. 3C). Weeks 4 and 12 were the two expression peaks. The data also showed that the level of HO-1 mRNA decreased at week 6, compared to week 4 ($P = 0.017$).

We used immunofluorescence to determine the types of cells responsible for the changes in HO-1 expression in the retinas of diabetic rats. A very small quantity of HO-1 expression was observed in the normal control retinas, mainly in the inner nuclear layer (INL; Figs. 4A, 4G). At week 2, HO-1 immunoactivity increased in the RGC layer and INL of diabetic retinas, with weak expression in the inner plexiform layer (IPL, Fig. 4B). At week 4, the expression increased further in the RGC layer, INL, and IPL, and appeared more intensely in the Müller cell nucleus and the processes crossing the whole retina, including the outer nuclear layer (ONL). The configuration of the Müller cells could be identified (Figs. 4C, 4D, 4H). Compared to week 4, the immunoactivity decreased in the RGC layer and INL at week 6 (Fig. 4E). In the diabetic retinas, at week 12, HO-1 immunoactivity increased in the RGC layer and IPL, compared to week 6 (Figs. 4F, 4I; $n = 6$).

Effect of Hemin on Expression of HO-1 in the Retinas of Diabetic Rats

In Figures 5A and 5B, Western blot analysis showed that the expression of retinal endogenous HO-1 was barely detectable after saline injection in the vehicle group, and elevated at 4 and 8 weeks in the blank group ($P < 0.0001$ and $P = 0.0023$ at weeks 4 and 8, respectively; $n = 6$). The hemin-induced expression of HO-1 in diabetic retinas was significantly higher than that in the nontreated blank group at week 8 (therapy group versus blank group, 5.06 ± 1.32-fold vs. 4.83 ± 0.59-fold at week 4 and 3.21 ± 0.51-fold vs. 1.02 ± 0.04-fold at week 8; $P = 0.7658$ and $P = 0.0011$ at weeks 4 and 8, respectively; $n = 6$). There was no significant difference between the vehicle and normal groups ($P = 0.235$). Consistent with the protein data, quantitative real-time PCR revealed a significant elevation of HO-1 mRNA in the diabetic blank group, compared to the control group (Fig. 5C; $P = 0.0127$ and $P = 0.0035$ at weeks 4 and 8, respectively; $n = 6$) and a significant elevation of the hemin-induced expression of HO-1 mRNA at week 8, compared to the blank group ($P = 0.0632$ and $P = 0.0009$ at weeks 4 and 8, respectively). The vehicle group had no significant difference compared to the normal group ($P = 0.615$)

Immunofluorescence analysis showed that the intraperitoneal injection of hemin induced prominent expression of HO-1 in the retinas of diabetic rats at week 8 (Fig. 6). The expression occurred mainly in the IPL, INL, and ONL, and especially in the RGC layer (Fig. 6C). By contrast, moderate HO-1 expression was observed at week 8 in the RGC layer, INL, and IPL of the untreated diabetic blank group (Fig. 6B). Immunoactivity of HO-1 was barely detectable in the vehicle retina, except weak expression in the INL (Fig. 6A, $n = 6$)..

Effect of Hemin on the Expression of Nrf2 and Activation of ERK 1/2 in the Retinas of Diabetic Rats

Western blot analysis determined that the level of retinal Nrf2 expression rose after diabetes was induced and peaked at week 4 (Figs. 7A, 7B). The second expression peak was at week 12 ($P = 0.0026$, $P = 0.0056$, $P = 0.0045$, $P = 0.0182$, and $P = 0.0024$ at weeks 2, 4, 6, 8, and 12, respectively; $n = 6$). We detected the active Nrf2 at approximately 90 kDa. The hemin-induced expression of Nrf2 in diabetic retinas was significantly

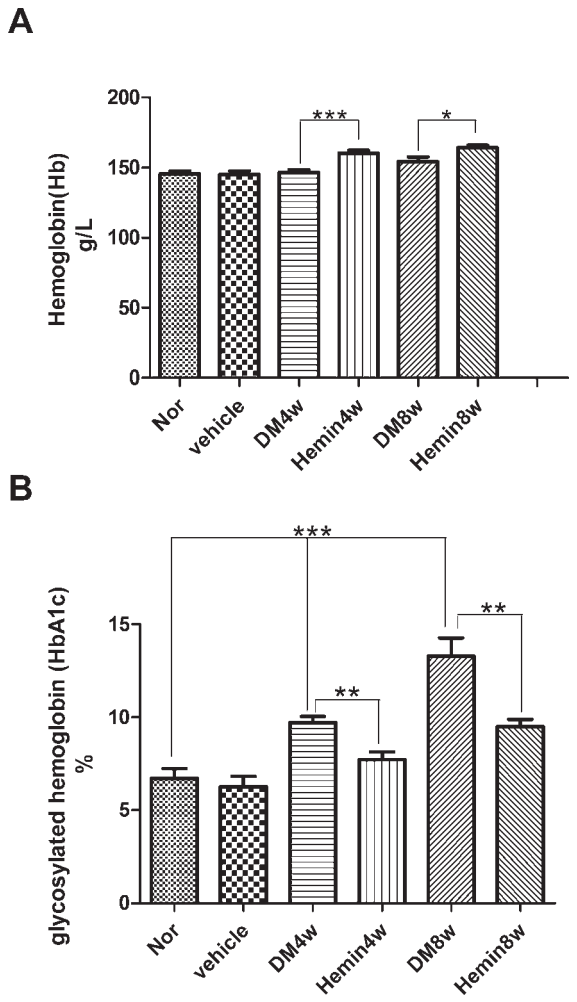

Figure 2. (**A**) The mean blood Hb levels were significantly higher in rats in the hemin-treated groups after hemin administration every other day (***$P < 0.001$ at week 4 and *$P < 0.05$ at week 8, $n = 10$) than the levels in the diabetic blank groups. (**B**) The mean blood HbA1c levels of the diabetic group gradually rose (***$P < 0.001$, $n = 10$), and HbA1c level in two hemin-treated time points were significantly lower than that of two diabetic blank time points (**$P < 0.01$ at weeks 4 and 8, $n = 10$).

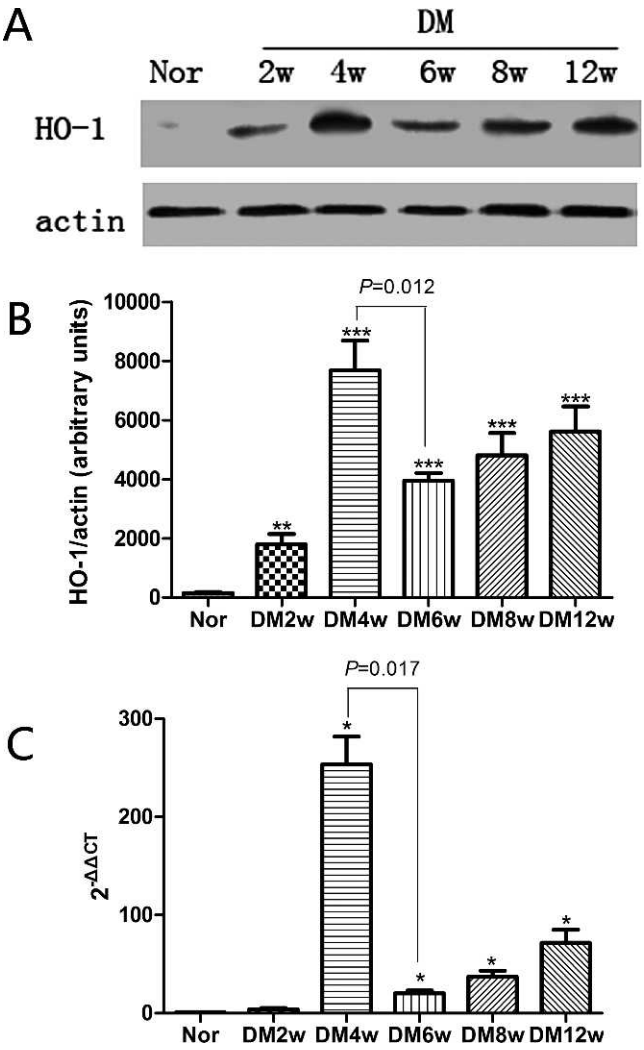

Figure 3. (**A**) Western blot analysis for expressions of HO-1 after onset of diabetes. (**B**) Quantitative analysis of expression of HO-1 protein in diabetic rat retinas and normal retinas. Expression of HO-1 was presented as expression density against values of actin. *Asterisks*: groups significantly different from normal control group (**$P < 0.01$, ***$P < 0.001$, $n = 6$). Expression of HO-1 was strikingly descended at week 6 compared to week 4 ($P = 0.012$). (**C**) Expression of HO-1 mRNA determined by real-time PCR. Values were standardized to β-actin mRNA levels and calculated as $2^{-\Delta\Delta C_T}$ in the same RNA samples. *Asterisks*: groups significantly different from normal control group (*$P < 0.05$, $n = 6$). Expression of HO-1 mRNA was strikingly decreased at week 6 compared to week 4 ($P = 0.017$).

higher than the expression in the nontreated blank group (therapy group versus blank group 3.23 ± 0.46-fold vs. 2.30 ± 0.36-fold at week 4 and 3.95 ± 0.50-fold vs. 1.59 ± 0.25-fold at week 8; $P = 0.003$ at weeks 4 and 8). At various intervals after STZ-induced high blood glucose (2, 4, 6, 8, and 12 weeks), the protein level of total ERK1/2 (tERK) was unchanged (Fig. 7C, $P = 0.057$, $n = 6$) either in the hemin(+) therapy group ($P = 0.721$). In contrast, it was significantly higher in levels of phosphorylated ERK1/2 isoforms, compared to the normal control (Fig. 7C; $P = 0.0048$, $P = 0.0074$, $P = 0.0049$, $P = 0.1434$, and $P = 0.2408$ at weeks 2, 4, 6, 8, and 12, respectively; $n = 6$) and peaked at week 4. The time course and magnitude of increased ERK1/2 phosphorylation were similar to trends in the expression of HO-1 and Nrf2 (Figs. 3, 7B).The hemin-induced expression of pERK in diabetic retinas at week 8 was significantly higher than in the diabetic blank group (therapy group versus blank group 3.87 ± 0.46-fold vs. 0.94 ± 0.06-fold, $P = 0.0008$). Interestingly, the expression of pERK in the hemin(+) therapy group at week 4 had no marked tendency, compared to the diabetic blank group (therapy group versus blank group 2.84 ± 0.38-fold vs. 2.84 ± 0.57-fold, $P = 0.997$), but was significantly higher than in the normal group ($P = 0.0023$).

Immunofluorescence analysis of retinal tissues revealed that the Nrf2 protein was induced in the retinal RGC layer and IPL 4 weeks after onset of diabetes, and that activation of Nrf2 protein increased in the hemin-treated retina in the RGC layer, IPL, and INL (Figs. 8A, 8D, 8G, 8J, 8M). Phosphorylated ERK1/2 immunofluorescence in vehicle retinas showed hardly any immunoactivity (Fig. 8B). In diabetic retinas at weeks 4 and 8, labeling occurred mostly in the Müller cell nucleus and processes (Figs. 8E, 8H). A further increase in staining intensity occurred in the same pattern after hemin was inducted into the retinas of diabetic rats. The induced ERK1/2 phosphorylation increased mostly in the INL and RGC layer (Figs. 8K, 8N).

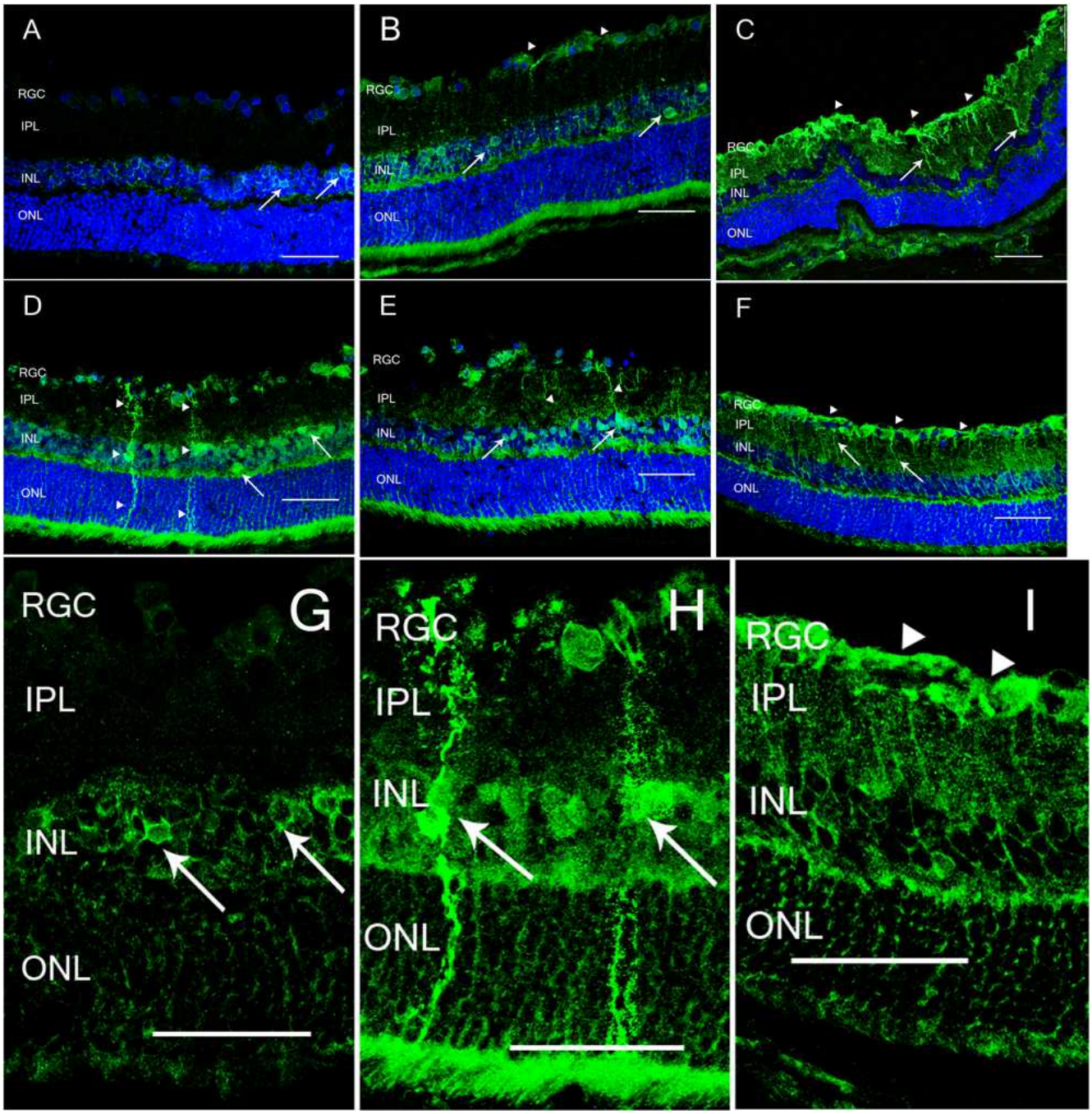

Figure 4. Immunofluorescence for localization of HO-1 protein. HO-1 immunoactivity (*green*) was detected by Alexa Fluor 488-labeled secondary antibody. Cell nuclei (*blue*) were counterstained with DAPI. (**A**) Normal retina. *Arrows*: weak HO-1 immunoactivity was detected in INL. (**B**) STZ-induced diabetic retina at week 2. *Arrows*: moderate HO-1 immunoactivity was detected in INL. *Triangles*: HO-1 immunoactivity was detected in RGC layer. (**C**) STZ-induced diabetic retina at week 4. Increased HO-1 immunoactivity was detected in INL, IPL (*arrows*) and RGC layer (*triangles*). (**D**) STZ-induced diabetic retina at week 4. Endogenous HO-1 immunoactivity was distributed in INL (*arrows*) and Müller cell nucleus, and processes crossing the whole retina (*triangles*). (**E**) STZ-induced diabetic retina at week 6. HO-1 immunoactivity was detected mainly in INL (*arrows*) and IPL (*triangles*). (**F**) STZ-induced diabetic retina at week 12. HO-1 immunoactivity was detected mainly in INL, IPL (*arrows*), and RGC layer (*triangles*). (**G**) Enlarged image of (**A**) without nuclei counterstaining. *Arrows*: weak HO-1 immunoactivity in INL. (**H**) Enlarged image of (**D**) without nuclei counterstaining. *Arrows*: HO-1 immunoactivity showed Müller cell configuration. (**I**) Enlarged image of (**F**) without nuclei counterstaining. *Triangles*: increased HO-1 immunoactivity in RGC layer. Original magnification (**A–F**) 400× and (**G–I**) 1200×, *scale bar* = 50 μm, $n = 6$.

Immunofluorescence Studies of GFAP Activation in Hemin Treated Diabetic Rat Retina

We observed activation of glial fibrillary acidic protein (GFAP) in retinas examined for immunohistochemical staining at 4 and 8 weeks after the induction of diabetes and hemin treatment (Fig. 8). The induced expression of GFAP was detected in the inner limiting membrane (ILM), RGC layer, and IPL, indicating the activation of macroglia, including astrocytes and Müller cells (Figs. 8L, 8O). In contrast, immunoactivity of the GFAP was detected at weeks 4 and 8 only in the ILM and RGC layer in

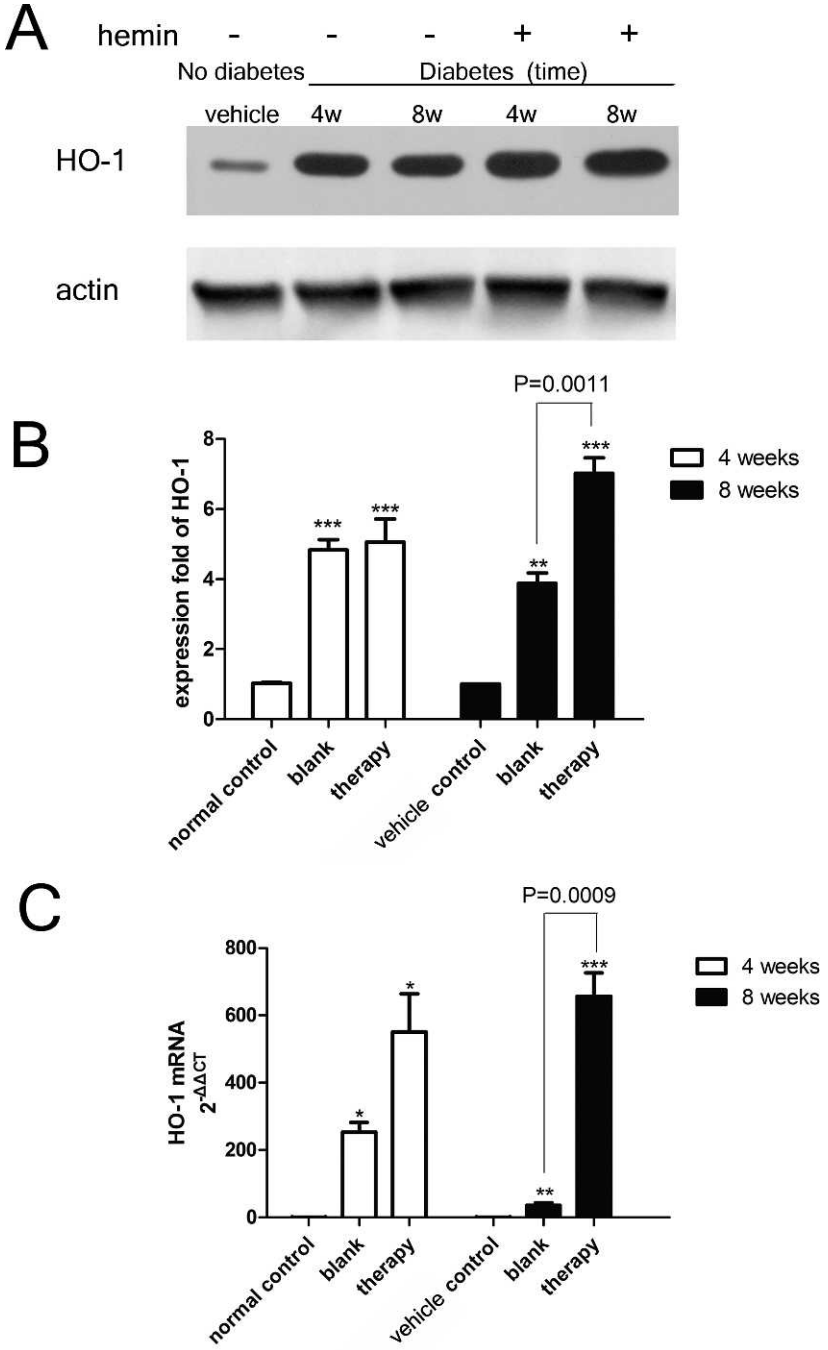

Figure 5. (**A**) Western blot analysis for expressions of HO-1 after administration of hemin. Retina tissues with physiologic saline treatment as vehicle group also were analyzed by Western immunoblotting. (**B**) The Western blot results are presented as expression fold of HO-1 activation, normalized against values of actin controls to adjust for protein loading. Normal group and vehicle group were both control groups. *Asterisks*: blank and therapy groups that were significantly different from control group at different time points ($^{**}P < 0.01$, $^{***}P < 0.001$, $n = 6$). (**C**) Expression of HO-1 mRNA determined by quantitative real-time PCR. *Asterisks*: blank and therapy groups that were significantly different from control group at different time points ($^{*}P < 0.05$, $^{**}P < 0.01$, $^{***}P < 0.001$, $n = 6$).

the vehicle group, and increased staining intensity in the same layers of the nontreated diabetic retinas (Figs. 8C, 8F, 8I; $n = 5$ eye samples at each time-point in each group).

Effect of Hemin on Expression of HIF-1α, SOD-1, mRNA, and Protein in the Retinas of Diabetic Rats

To document the inhibitory effect of induced HO-1 on retinal oxidative injury after high diabetic levels of glucose, we investigated the expressions of HIF-1α and SOD-1. In Figures 9A, 9B, and 9D, Western blot analysis showed that initially the expressions of retinal endogenous HIF-1α and SOD-1 were barely detectable in the vehicle group, but were significantly higher when measured at 4 and 8 weeks after diabetes was induced (HIF-1α $P = 0.0033$ at week 4 and $P = 0.0018$ at week 8; SOD-1, $P < 0.0001$ at week 4 and $P = 0.0023$ at week 8; $n = 6$). The hemin injection reduced the expression of HIF-1α in diabetic retinas at weeks 4 and 8 (therapy group versus blank

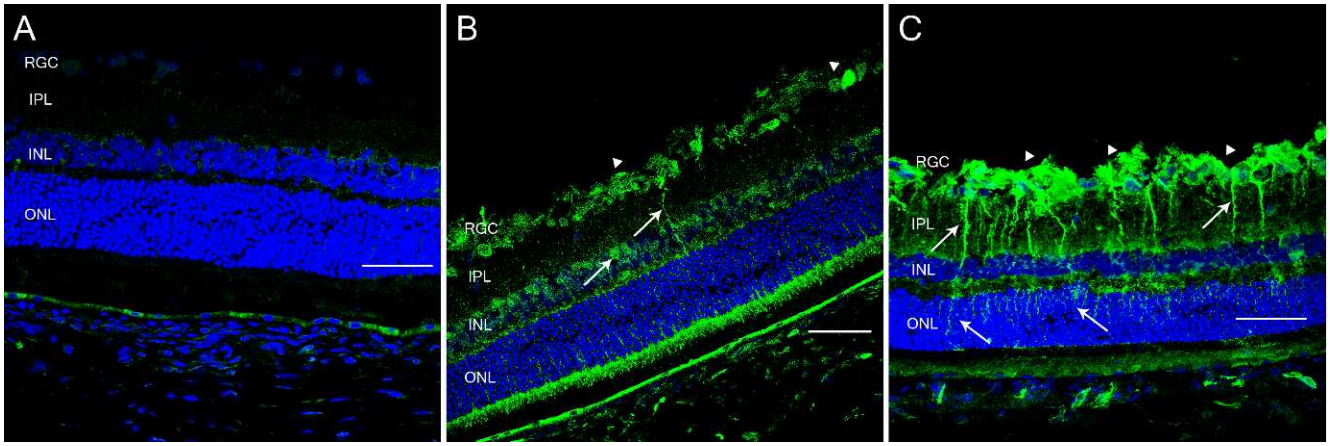

Figure 6. Immunofluorescence for localization of hemin-induced HO-1 protein. (**A**) Intraperitoneal saline-treated rat retina in vehicle group. (**B**) STZ-induced diabetic retina without treatment at week 8 (blank group). *Arrows*: moderate HO-1 immunoactivity was detected in INL and IPL. *Triangles*: HO-1 immunoactivity was detected in RGC layer. (**C**) Hemin-treated diabetic rat retina at week 8 (therapy group). Markedly increased HO-1 immunoactivity was detected in INL, IPL, ONL (*arrows*), and RGC layer (*triangles*). Original magnification 400×, *scale bar* = 50 μm, $n = 6$.

group, 18.92 ± 5.62-fold vs. 33.23 ± 13.65-fold at week 4 and 24.94 ± 9.78-fold vs. 40.78 ± 7.57-fold at week 8; $P = 0.0411$ and $P = 0.0429$ at weeks 4 and 8, respectively), indicating that the induction of HO-1 suppressed the expression level of HIF-1α protein. In contrast, the expression level of SOD-1 was significantly higher in hemin(+) diabetic retinas compared to the hemin(−) blank group (therapy group versus blank group, 6.87 ± 1.29-fold vs. 4.73 ± 0.57-fold at week 4 and 9.83 ± 2.67-fold vs. 5.17 ± 0.86-fold at week 8; $P = 0.0228$ and $P = 0.0159$ at weeks 4 and 8, respectively). It is possible that overexpression of HO-1 might have a contribution to activation of SOD-1.

As shown in Figures 9C and 9E, quantitative real-time PCR revealed a significant reduction in the expression of HIF-1α mRNA in the retinas of hemin-treated rats ($P = 0.0051$ and $P = 0.0031$ at weeks 4 and 8, respectively; $n = 6$), and a significant elevation of the hemin-induced expression of SOD-1 mRNA ($P = 0.0095$ and $P = 0.0176$ at weeks 4 and 8, respectively), compared to the diabetic blank group. HIF-1α mRNA and SOD-1 mRNA levels were significantly higher in the diabetic blank group than in the control group (HIF-1α, $P = 0.0237$ and $P = 0.0016$ at weeks 4 and 8, respectively; SOD-1, $P = 0.0404$ and $P = 0.0744$ at weeks 4 and 8, respectively).

Effect of Hemin on Expression of VEGFa mRNA and Protein in Retinas of Diabetic Rats

As shown in Figures 10A and 10B, the densitometry of the VEGF immunoreactive band of approximately 25 kDa was significantly higher at 4 and 8 weeks after the injection of STZ to induce diabetes than in the control group ($P < 0.0001$ and $P = 0.0002$ at weeks 4 and 8, respectively, $n = 6$). This elevation in the level of VEGF protein was attenuated significantly in the retinas of hemin-treated rats at 4 weeks of diabetes (therapy group versus blank group, 7.57 ± 2.23-fold vs. 9.50 ± 2.09-fold at week 4 and 8.85 ± 2.13-fold vs. 10.17 ± 3.22-fold at week 8; $P = 0.0321$ and $P = 0.1234$ at weeks 4 and 8, respectively). Consistent with the protein data, our analysis revealed higher level of VEGFa mRNA in the diabetic blank group, compared to the control group (Fig. 10C; $P = 0.0138$ and $P = 0.0043$ at weeks 4 and 8, respectively; $n = 6$) and reduced expression of VEGFa mRNA in the hemin(+) therapy group, compared to the blank group (Fig. 10C; $P = 0.0277$ and $P = 0.0224$ at weeks 4 and 8, respectively), suggesting the direct role of HO-1 in the inhibition of VEGF.

Hemin-Mediated Suppression of p53 and Activation of bcl-2 in the Retinas of Diabetic Rats

To capture the anti-apoptotic effect of the hemin-induced expression of HO-1 in the retinas of diabetic rats, the expressions of p53 and survival-promoting bcl-2 were detected. As shown in Figures 11A and 11B, Western blot analysis revealed that the expression of retinal p53 protein was nearly undetectable in the vehicle group, and was significantly higher at 4 and 8 weeks after diabetes was induced than in the vehicle group ($P < 0.0001$, $n = 6$). Hemin therapy reduced the expression of p53 in the retinas of diabetic rats at weeks 4 and 8 (therapy group versus blank group, 1.17 ± 0.30-fold vs. 3.49 ± 0.40-fold at week 4 and 1.89 ± 0.49-fold vs. 3.67 ± 0.18-fold at week 8; $P < 0.0001$), indicating that hemin treatment delayed the expression of p53. In contrast, expression of bcl-2 was detected in the vehicle group and was significantly lower in the hemin(−) diabetic blank group (Figs. 11A, 11D; $P = 0.0011$). A higher level of expression of the bcl-2 protein was detected in the retinas of hemin-treated rats, compared to the diabetic blank group (therapy group versus blank group, 1.05 ± 0.08-fold vs. 0.81 ± 0.17-fold at week 4 and 1.14 ± 0.17-fold vs. 0.41 ± 0.03-fold at week 8; $P < 0.0001$), indicating induced HO-1 might have a contribution to activation of bcl-2.

Figures 11C and 11E show that quantitative real-time PCR revealed significantly higher expression of p53 mRNA ($P < 0.0001$, $n = 6$) and a significant reduction in the expression of bcl-2 mRNA ($P = 0.0005$) in the nontreated diabetic blank group, compared to the vehicle group. We also found a significant attenuation in the p53 mRNA expression from the retinas of the hemin-treated rats ($P < 0.0001$), compared to the diabetic blank group. The hemin-induced expression of bcl-2 mRNA was significantly higher in the therapy group than in the blank group ($P = 0.0001$). The expression levels of p53 and bcl-2 mRNA were similar to trends in the expression of p53 and bcl-2 protein.

Effect of Hemin on Protection of Retinal Ganglion Cells

To determine the neuroprotective effect of hemin in diabetic retinas, we counted the number of TUNEL-positive cells in RGC layer. We also counted the number of dil-labeled RGCs.

Obvious TUNEL-positive nuclei were found in the RGC layer at 8 weeks after diabetes was induced (Fig. 12). However, the

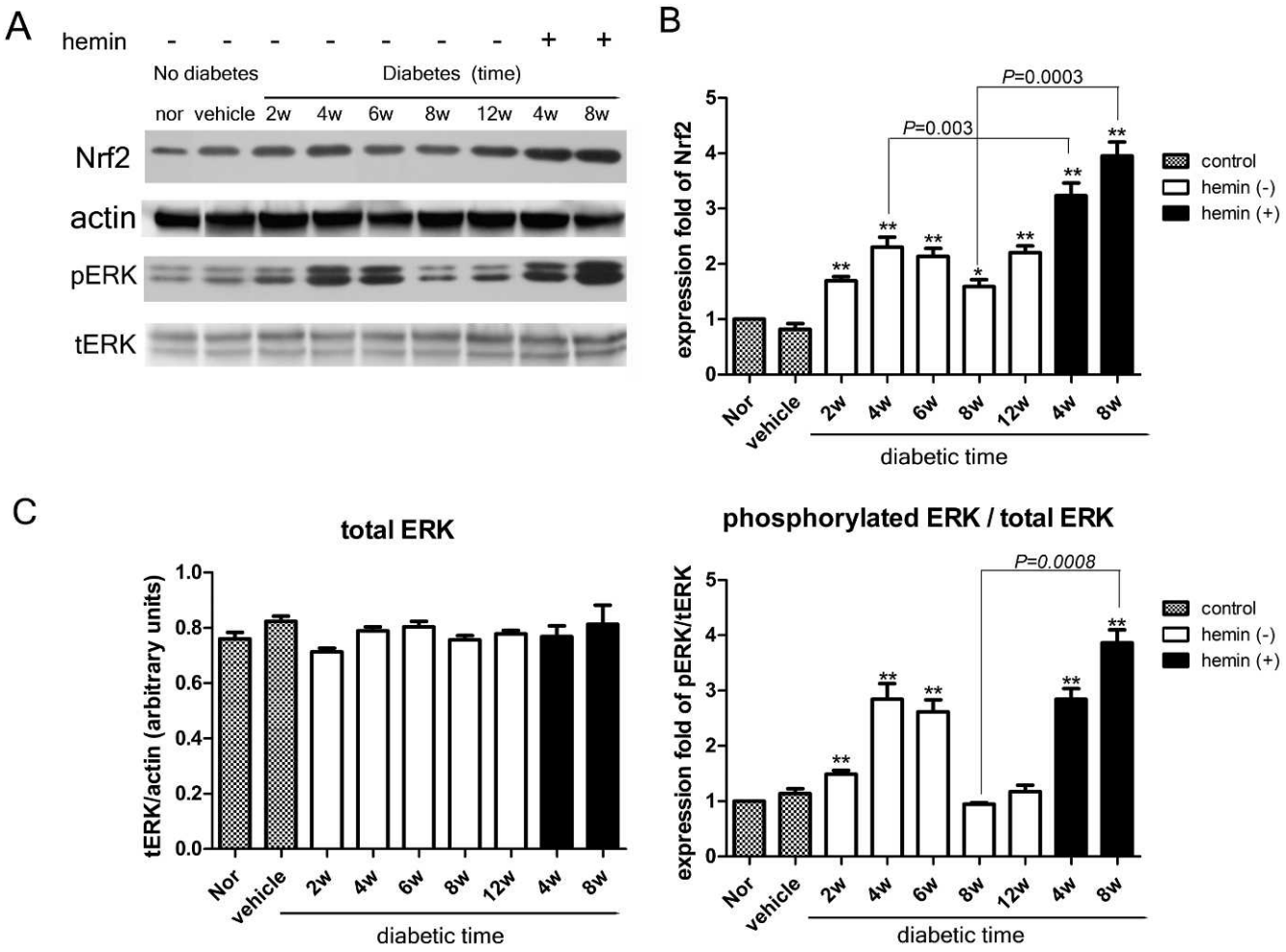

Figure 7. (**A**) Western blot analysis for expressions of Nrf2, total ERK 1/2 (tERK), and phosphorylated ERK 1/2 (pERK) after onset of diabetes and administration of hemin. (**B**) Quantitative analysis of expression of Nrf2 protein in diabetic rat retinas and control retinas. The Western blot results are presented as expression fold of Nrf2 activation, normalized against values of actin controls to adjust for protein loading. *Asterisks*: groups that were significantly different from normal control group ($^*P < 0.05$, $^{**}P < 0.01$, $n = 6$). Expression of Nrf2 was significantly higher in hemin(+) group than hemin(–) group ($P = 0.003$ at weeks 4 and 8). (**C**) Quantitative analysis of expression of tERK and pERK isoform in diabetic rat retinas and control retinas. In diabetic retinas, at time points of the study (2, 4, 6, 8, and 12 weeks), the total levels of ERK1/2 isoform were unchanged. The phosphorylated levels of ERK1/2 isoform are presented as expression fold of pERK/tERK ratio. *Asterisks*: groups that were significantly different from normal control group ($^{**}P < 0.01$, $n = 6$). Expression of pERK was significantly higher ($P = 0.0008$ at week 8) in hemin(+) group compared to the hemin(–) group.

apoptotic cells in the RGC layer of diabetic rats was significantly reversed by hemin. In Figure 12B, a quantitative analysis of the number of TUNEL-positive nuclei in the RGC layer shows that there were statistically fewer apoptotic cells in hemin-treated retinas (5.28 ± 1.53 and 12.32 ± 2.80 cells/1.0 mm length at weeks 4 and 8, respectively;) than in nontreated blank retinas (6.00 ± 1.66 and 28.72 ± 4.37 cells/1.0 mm length at weeks 4 and 8, respectively, $P < 0.0001$, $n =$ 6 eye samples at each time-point in each group). Interestingly, a certain number of apoptotic cells in INL also was found in the retinas of diabetic rats and reduced after hemin treatment (Fig. 12A). These cells could be apoptotic Müller cells. But we didn't do the verification or the quantitative analysis in this paper.

The numbers of dil-labeled RGCs at weeks 4 and 8 in the normal, blank and therapy groups are shown in Table 3 ($n = 6$ eye samples at each time-point in each group). The mean number of labeled RGCs in the normal retinas was 2472 ± 145 cells/mm^2 (no significant difference was found among all the time-points in normal group, $P = 0.911$). After diabetes was induced, the mean densities of dil-labeled RGCs reduced to 2282 ± 105 cells/mm^2 at week 4 ($P < 0.05$) and 2001 ± 207 cells/mm^2 at week 8 ($P < 0.01$). After hemin therapy, the mean number was 2318 ± 114 cells/mm^2 at week 8. This is significantly higher than that in blank group at week 8 ($P <$ 0.01).

Discussion

Recently, a great deal of evidence has indicated the critical importance of upregulating HO-1 in mediating anti-inflammatory, anti-oxidant, anti-apoptotic, and anti-proliferative effects. The overexpression of HO-1 by pharmacologic modulation or gene transfer may represent a novel strategy for therapeutic intervention in the future.[28–32]

In this study, we observed an increased concentration of blood hemoglobin and the decrease of glycosylated blood hemoglobin in diabetic rats after hemin treatment. We also found that the levels of expressed HO-1 protein and mRNA in retinal tissue after diabetes was induced followed the same time course and magnitude as the trends in the expression of

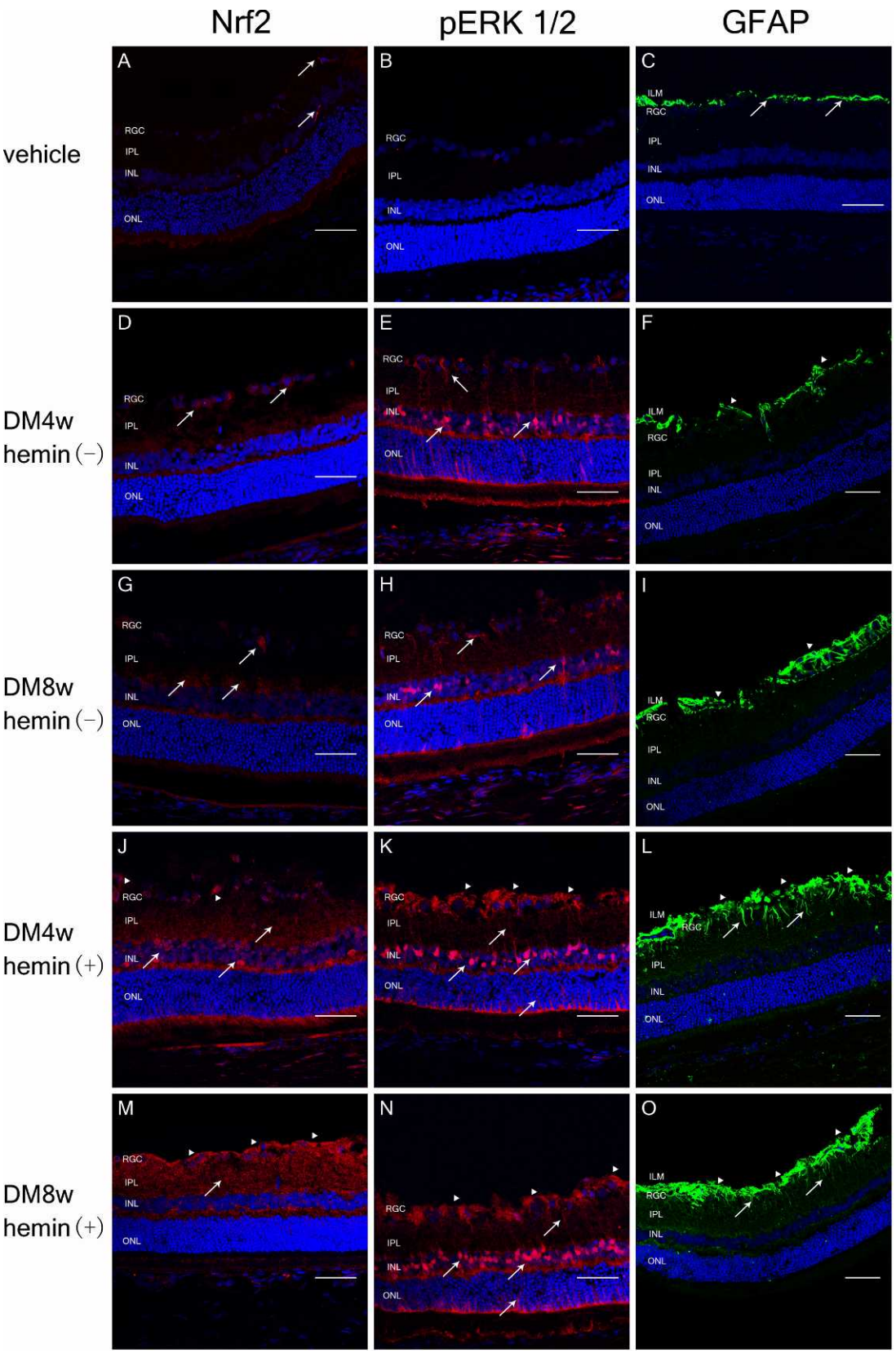

Figure 8. Immunofluorescence for localization of Nrf2, pERK 1/2 and GFAP protein. Nrf2 and pERK 1/2 immunoactivity (*red*) was detected by Alexa Fluor 555-labeled secondary antibody. GFAP immunoactivity (*green*) was detected by Alexa Fluor 488-labeled secondary antibody. Cell nuclei (*blue*) were counterstained with DAPI. (**A**) Vehicle control retina. *Arrows*: weak Nrf2 immunoactivity was detected in RGC layer and INL. (**D**, **G**) Expression of Nrf2 in hemin(–) diabetic rat retina. *Arrows*: moderate Nrf2 expression was detected in RGC layer and INL. (**J**, **M**) Expression of Nrf2 in hemin(+) diabetic rat retina. *Arrows*: induced Nrf2 immunoactivity was detected in IPL and INL. *Triangles*: induced Nrf2 immunoactivity in RGC layer. (**B**) Vehicle control retina. There was little expression of pERK1/2. (**E**, **H**) Expression of pERK 1/2 in hemin(–) diabetic rat retina. *Arrows*:

pERK 1/2 immunoactivity was detected in RGC layer, INL, and Müller cell processes. (**K**, **N**) Expression of pERK 1/2 in hemin(+) diabetic rat retina. Induced pERK ½ immunoactivity was markedly increased in INL, IPL, ONL (*arrows*), and RGCs (*triangles*). (**C**) Vehicle control retina. *Arrows*: GFAP immunoactivity was detected in ILM. (**F**, **I**) Expression of GFAP in hemin(−) diabetic rat retina. *Triangles*: increased GFAP activation was detected in ILM and RGC layer. (**L**, **O**) Expression of GFAP in hemin(+) diabetic rat retina. Induced GFAP immunoactivity was markedly ascended in ILM and RGC layer (*triangles*) and detected in IPL (*arrows*). Original magnification 400×, *scale bar* = 50 μm, $n = 6$.

Nrf2 and phosphorylated ERK1/2 (Figs. 3, 7). Additionally, our study revealed that after hemin treatment, a strong upregulation of HO-1 in the retinal RGC layer, IPL, INL, and ONL (Figs. 5, 6) are combined with activation of the Nrf2/ERK pathway (Fig. 7) and attenuated apoptosis in the RGCs (Fig. 12, Table 3) in the diabetic retina. This observation suggests that pharmacologically inducing overexpression of HO-1 in the retina by administering hemin could provide protection against neuron degeneration from diabetes. Meanwhile, treatment with hemin also induced the antioxidant defense enzyme SOD-1 and the anti-apoptotic protein bcl-2 to overexpress in the retina of diabetic rats (Figs. 9, 11). On the other hand, hemin treatment significantly attenuated the expression of HIF-1α, VEGF, and P53 (Figs. 9–11). These results indicated that the protective effect of HO-1 may occur in part through the induction of SOD-1 and bcl-2, and inhibition of HIF-1α, VEGF, and P53.

Recent studies have demonstrated that redox-sensitive transcription factor Nrf2 responds to inflammatory stimuli and rescues cells/tissues from inflammatory injuries through its capacity to induce the expression of antioxidant enzymes,

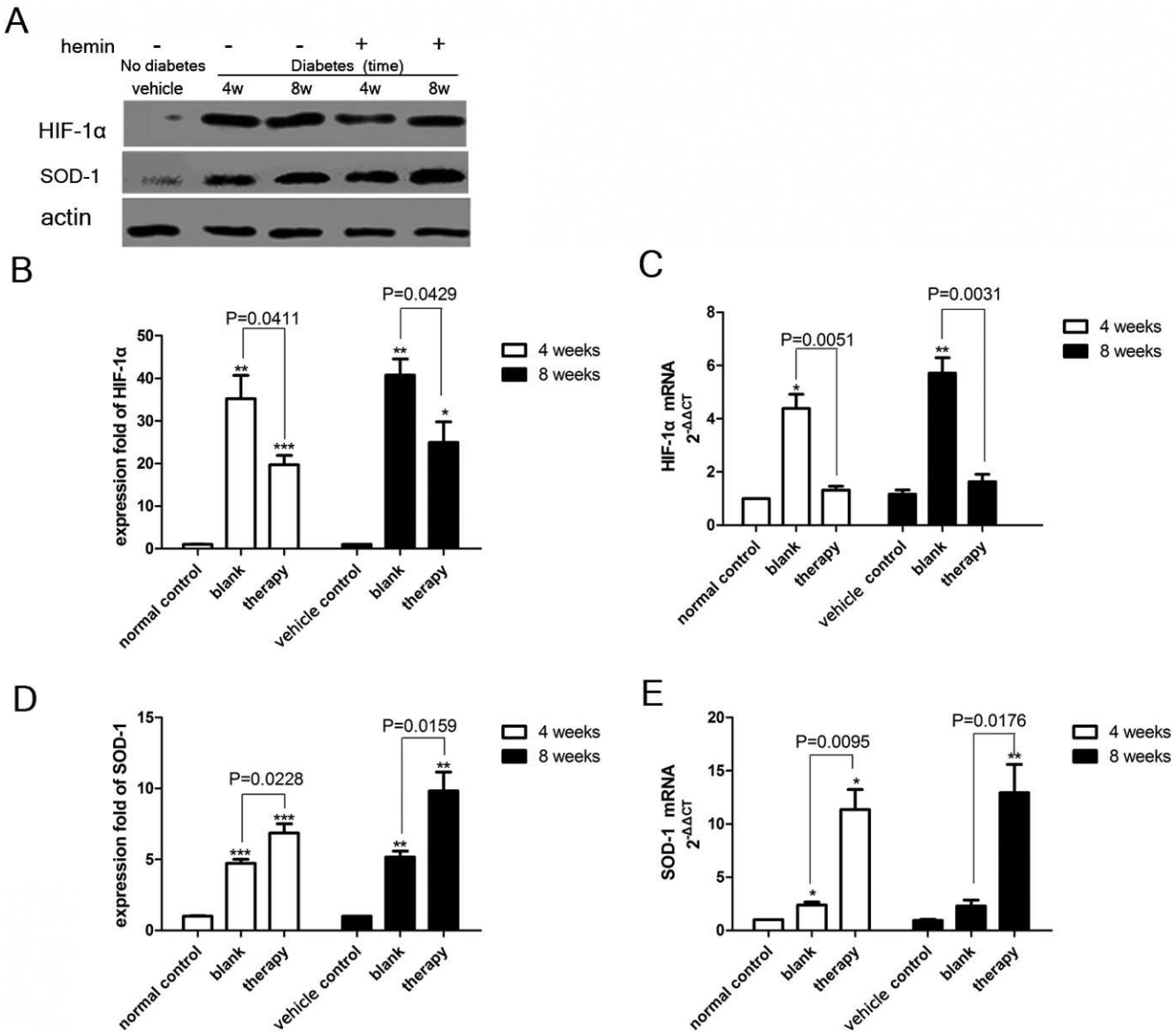

Figure 9. (**A**) Western blot analysis for expressions of HIF-1α and SOD-1 after administration of hemin. (**B**, **D**) The Western blot results are presented as expression fold of HIF-1α and SOD-1, normalized against values of actin controls to adjust for protein loading. *Asterisks*: blank group and therapy group that were significantly different from control group at different time points ($^*P < 0.05$, $^{**}P < 0.01$, $^{***}P < 0.001$, $n = 6$). (**C**, **E**) Expression of HIF-1α and SOD-1 mRNA determined by quantitative real-time PCR. *Asterisks*: blank group and therapy group that were significantly different from control group at different time points ($^*P < 0.05$, $^{**}P < 0.01$, $^{***}P < 0.001$, $n = 6$).

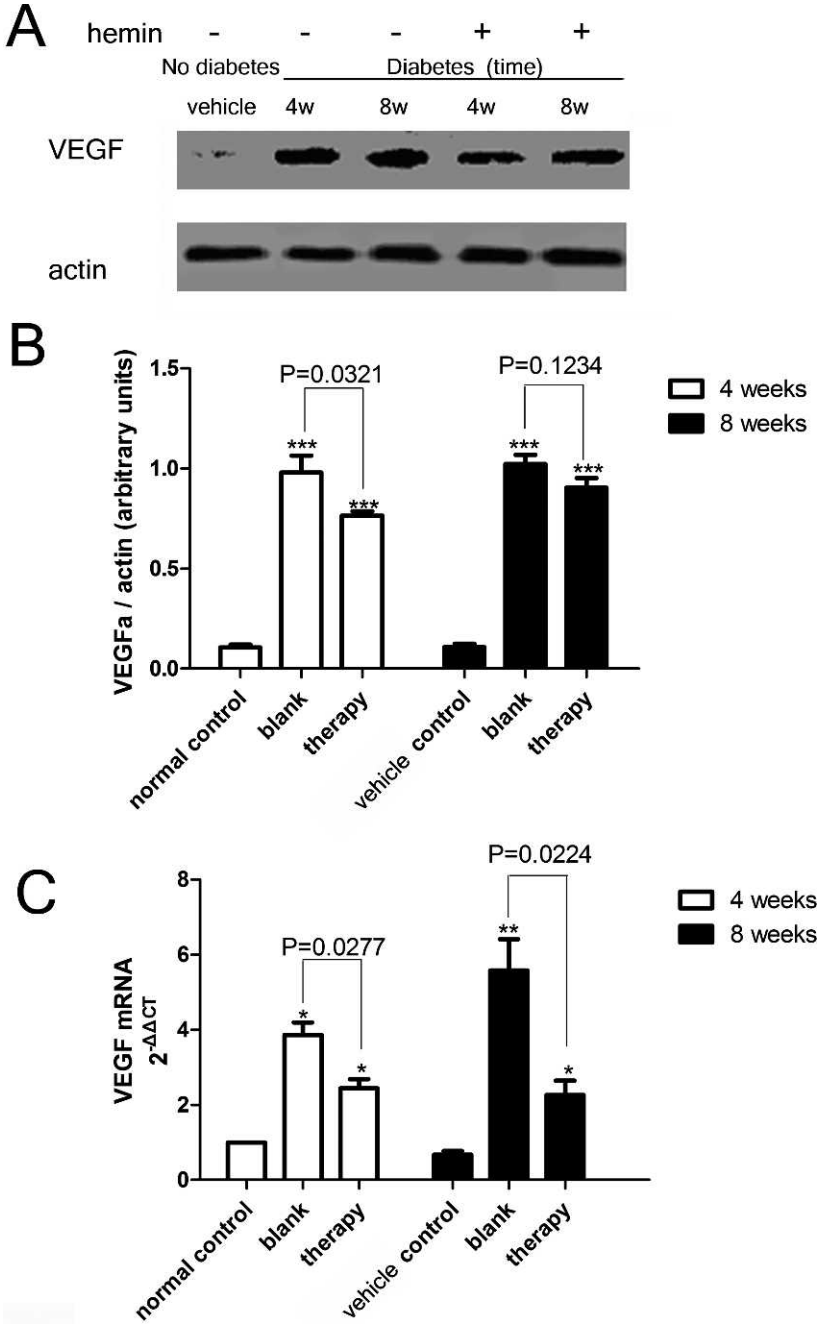

Figure 10. (**A**) Western blot analysis for expressions of VEGFa in hemin-treated and nontreated retinas. (**B**) The Western blot results of VEGFa are presented as expression density against values of actin. *Asterisks*: blank group and therapy group that were significantly different from control group at different time points (***$P < 0.001$, $n = 6$). (**C**) Expression of VEGFa mRNA determined by quantitative real-time PCR. *Asterisks*: blank group and therapy group that were significantly different from control group at different time points (*$P < 0.05$, **$P < 0.01$, $n = 6$).

including HO-1.[22,33] To our knowledge, the exact role of Nrf2 in the retina in response to diabetic injury and HO-1 induction has not been clarified. Our results demonstrated that the expression level of Nrf2 and phosphorylated ERK1/2 was upregulated 2 weeks after diabetes was induced by STZ and peaked at 4 weeks, which coincides with the peak of HO-1 expression in the retinas of diabetic rats (Fig. 7). We also found that the expression of Nrf2 and phosphorylated ERK1/2 was increased after hemin treatment. These data imply that ERK1/2 may be the candidate kinase to activate Nrf2 nuclear translocation and subsequently induce HO-1 expression.

Müller cells, spanning the entire retinal thickness, are known for the importance of their physiologic function and pathologic resistance to insults to the retina: local pH shifts, excitotoxic reactions, generation of oxygen free radicals, and neurotrophic factors in the diabetic retina.[34,35] The activation of Müller cells is the retina's anti-stress, self-protection reaction. Our immunohistochemical studies indicated that HO-1 was expressed selectively in the nucleus and processes of Müller cells, and that expression from the retinas of diabetic rats was found in all parts of the Müller cell, from the internal to the external limiting membrane (Fig. 4). Concurrently, the activation of pERK 1/2 was located mainly in the INL and the Müller cell processes. The

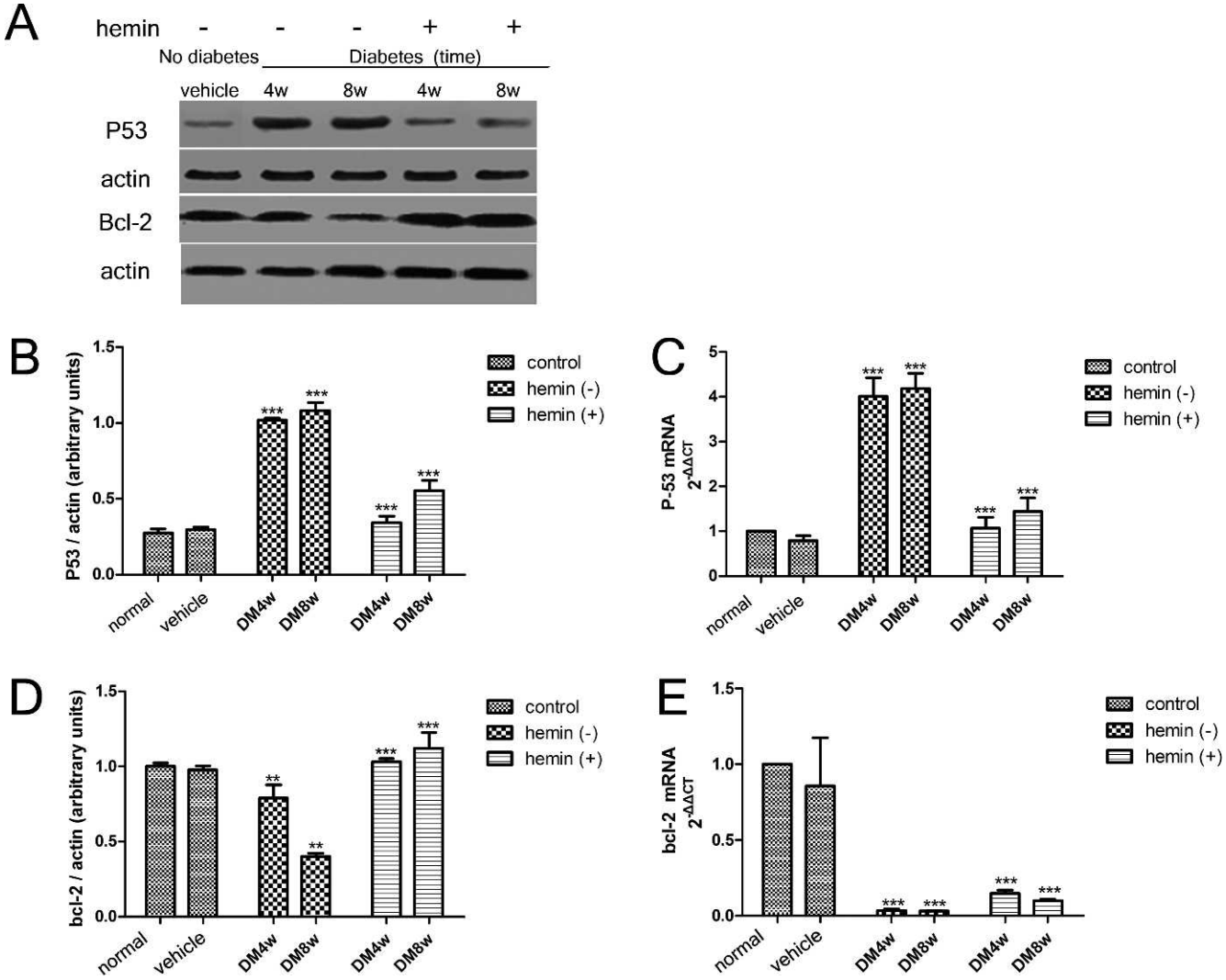

Figure 11. (**A**) Western blot analysis for expressions of p53 and bcl-2 in hemin-treated and nontreated retinas. (**B**, **D**) The Western blot results of p53 and bcl-2 are presented as expression density against values of actin. *Asterisks*: hemin(+) group that was significantly different from hemin (–) group, and hemin(–) group that was significantly different from control group (**$P < 0.01$, ***$P < 0.001$, $n = 6$). (**C**, **E**) Expression of p53 and bcl-2 mRNA determined by quantitative real-time PCR. *Asterisks*: hemin(+) group that was significantly different from hemin(–) group, and hemin(–) group that was significantly different from control group (***$P < 0.001$, $n = 6$).

hemin-induced immunoactivity of pERK 1/2 increased in the INL and RGC layer. The GFAP expression in the hemin-treated retinas of the diabetic rats was detected by increased staining intensity in RGC layer, ILM, and IPL, compared to the limiting expression in the ILM of retinas from untreated diabetic rats (Fig. 8). Our previous study in STZ-induced diabetic rats indicated that GFAP is expressed by astrocytes in the ILM in normal retinas and activated in diabetic retinas by the Müller glial end foot.[36] Our observation indicated that the mechanism behind protecting against diabetic injury to retina, involving GFAP expression, concurrent with HO-1 induction and pERK activation, is related to Müller cell activation rather than to modulation of other types of retinal cells.

As part of understanding how diabetes leads to pathologic changes in retinopathy, recent evidence suggests a key role for oxidative stress, a state in which excess reactive oxygen species (ROS), overwhelm endogenous antioxidant systems.[37] Superoxide dismutase (SOD) is an important gene in the ROS network; it catalyzes the dismutation of superoxide into O_2 and H_2O_2, serving a key antioxidant role.[38,39] The therapy that inhibits the development of retinopathy in diabetic rats prevents diabetes-induced increases in retinal superoxide accumulation and inhibition of SOD activity.[40] Overexpression of cytosolic SOD (Cu-Zn SOD, SOD-1) has been shown to attenuate diabetes-induced renal injury in streptozotocin-diabetic mice and db/db mice.[41,42] In our study, the results showed that the levels of this intracellular antioxidant were upregulated in the retina of diabetic rats at weeks 4 and 8. We presume it is a self-protective response at early stage of diabetic retinopathy, which is the same as increased level of HO-1 in the diabetic retina. We also found out that the overexpression of SOD-1 mRNA and protein were induced after hemin treatment. Our results suggested that hemin-induced HO-1 expression could provide retinal protection in the retinas of diabetic rats in part by SOD-1 induction.

Hypoxia is another risk factor that can accelerate the onset and progression of diabetic retinopathy.[43] The early changes provoked by hyperglycemia, including leukostasis, vasoconstriction, and a pro-inflammatory state, can cause hypoxia in the retina directly.[44] Hypoxia accelerates the inflammatory injury and neovascularization in the retina. Hypoxia-inducible factor 1α (HIF-1α) is sensitive to changes in the partial pressure

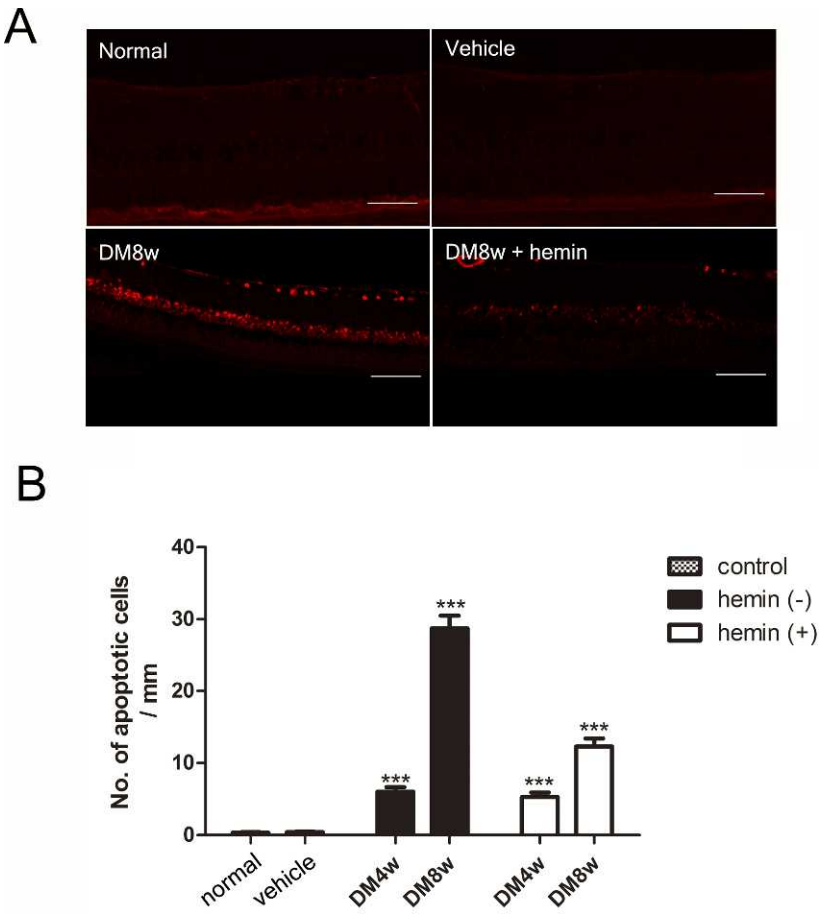

Figure 12. Antiapoptotic effect of HO-1. (**A**) Apoptosis in cells of RGC layer in each group was detected by TUNEL analysis. Original magnification 400×, *scale bar* = 100 μm, $n = 6$). (**B**) Quantitative analysis for number of TUNEL-positive cells in RGC layer. Data were expressed as the counting number of TUNEL-positive cells per millimeter field. *Asterisks*: hemin(+) therapy group that was significantly different from hemin(–) blank group (***$P < 0.001$), and hemin(–) blank group that was significantly different from control group (***$P < 0.001$).

of oxygen, and is a key regulator for cells adaptation to hypoxia and ischemia.[45] Under hypoxic conditions, the HIF-1α and HIF-1β heterodimerize to form the HIF-1 complex. VEGF and p53 are possible downstream genes regulated by HIF-1.[46,47] Thus, up-regulating HIF-1α could result in either promoting angiogenesis or suppressing cell survival in a hypoxic condition. Knockout of HIF-1α in Müller cells in mice attenuated the increases of retinal vascular leakage and adherent leucocytes, as well as the overproduction of VEGF and ICAM-1 under diabetic conditions.[48] These findings indicated that the activation of HIF-1α was associated with retinal inflammation and neovascularization. In our study, the retinal HIF-1α levels increased in the early stages of the rats' diabetes, and hemin decreased the expression of HIF-1α at weeks 4 and 8. This result raised the possibility that HO-1 could provide retinal protection in part by inhibiting the activation of HIF-1α.

Table 3. Number of RGCs/mm^2 4 and 8 Weeks after Hemin Injection in Diabetic Rats' Retinas

	Normal Group	Blank Group	Therapy Group
4 wk			
N	2448 ± 102	2282 ± 150	2306 ± 206
P value	–	0.0482*	0.8186
8 wk			
N	2518 ± 195	2001 ± 207	2318 ± 114
P value	–	0.0012†	0.0082†

Therapy group marked values were significantly different from hemin blank group. Blank group marked values were significantly different from normal group.

* $P < 0.05$.

† $P < 0.01$.

DR also is recognized as belonging to a group of neurodegenerative diseases that can be affected by progressive degeneration of RGCs.[49,50] The protooncogenic families of p53 and bcl-2 proteins are best known for their roles in cell death and survival: p53 is considered to promote cell apoptosis, while bcl-2 generally is considered to have an antiapoptotic role. Interestingly, overexpression of HO-1 promoted protection against tissue injury by altering the down regulated bcl-2 levels and upregulated p53 expression in a mouse model of ischemic stroke and HO-1 transgenic mutation.[51] In another study, HO-1 transgene expression, where photoreceptors mediated neuroprotection against light damage in a murine model, is correlated with a decrease in the expression of p53 and an increase in the activation of bcl-2.[12] As described in our study, in the retinas of untreated diabetic rats, the number of apoptotic RGCs increased at weeks 4 and 8. The mRNA and protein level of bcl-2 decreased and p53 increased. After hemin injection and HO-1 induction, we observed alterations in the expression of bcl-2 and p53, combined with a higher number of living RGCs. These alterations would be among the mechanisms by which increased expression of HO-1 promoted RGCs survival by activation of bcl-2 protein and inhibition of p53.

Apart from apoptosis, diabetic macular edema, retinal neovascularization, and proliferation also has occurred in the retina of a diabetic.[52,53] VEGF is a potent mitogen for endothelial cells, triggering the proliferation, migration, and tube formation that leads to growing new blood vessels.[54] In addition, VEGF induces leukocytes to adhere to the retinal vessels, following inflammatory injury, resulting in breaking down the blood-retinal barrier and leading to diabetic macular edema.[55,56] Clinical studies proved that intravitreal anti-VEGF drug injections, including the anti-VEGF aptamer, pegaptanib (Macugen; OSI Pharmaceuticals), the monoclonal antibody fragment Ranibizumab (Lucentis; Genentech Inc., San Francisco, CA), and the full length antibody bevacizumab (Avastin; Genentech Inc.), blocks VEGF-induced hyperpermeability of blood vessels and neovascularization.[56,57] To elucidate the anti-inflammation and anti-proliferation effect of HO-1, we evaluated the expression of VEGF protein and mRNA by the test rats. We demonstrated that the increase of VEGF protein and mRNA in the retina of diabetic rats could be attenuated by injecting hemin. It is possible that induced HO-1 expression could ameliorate inflammatory injury and prevent neovascularization by inhibiting the expression of VEGF.

The STZ-induced diabetic rat is one of the commonly used models of diabetes; the model displays morphologic and functional changes in the retina similar to those observed in the early stage of human DR.[58] HbA1c was recommended as a standard to diagnose for diabetes and stratify the risk, because its value represents the glycemic status over the last few months and it is well correlated with the complications of chronic diabetes.[59,60] Our result showed that hemin treatment significantly increased the mean blood Hb level in diabetic rats. Also, hemin treatment significantly reduced the elevated mean blood HbA1c level in diabetic rats. These results demonstrated that hemin possesses potential antidiabetic and antihyperglycemic qualities, and could benefit diabetes-induced retinal injury.

As the limitation of our study, we have limited evidence of cause-and-effect between hemin treatment and change of some markers in this report. Detection of these markers after we stop hemin treatment may be helpful to evaluate its effect. Furthermore, enzymatic assay, combined with expression detection by Western blotting and real-time PCR, could determine HO-1 activity better.

In conclusion, we demonstrated that expression of hemin-induced HO-1 resulted in upregulation of SOD-1 and bcl-2, as well as down-regulation of p53, VEGF, and HIF-1α. These effects attenuated diabetes-induced apoptosis in RGCs. The mechanism might work through the Nrf2/ERK signaling pathway. Hemin has a great potential to induce HO-1 expression in the retina of diabetes patients, and may have an important role for future therapeutic strategies to protect the retina neurons from the sort of inflammatory and oxidative stress-dependent damage observed during diabetic retinopathy.

References

1. Rungger-Brändle E, Dosso AA, Leuenberger PM. Glial reactivity, an early feature of diabetic retinopathy. *Invest Ophthalmol Vis Sci*. 2000;41:1971–1980.
2. Antonetti DA, Barber AJ, Bronson SK, et al. Diabetic Retinopathy Center Group. Diabetic retinopathy: seeing beyond glucose-induced microvascular disease. *Diabetes*. 2006;55:2401–2411.
3. Otterbein LE, Soares MP, Yamashita K, Bach FH. Heme oxygenase-1: unleashing the protective properties of heme. *Trends Immunol*. 2003;24:449–455.
4. Soares MP, Bach FH. Heme oxygenase-1: from biology to therapeutic potential. *Trends Mol Med*. 2009;15:50–58.
5. Zhang M, Zhang BH, Chen L, An W. Overexpression of heme oxygenase-1 protects smooth muscle cells against oxidative injury and inhibits cell proliferation. *Cell Res*. 2002;12:123–132.
6. Tamion F, Richard V, Renet S, Thuillez C. Intestinal preconditioning prevents inflammatory response by modulatinghemeoxygenase-1 expression in endotoxic shock model. *Am J Physiol Gastrointest Liver Physiol*. 2007;293:G1308–G1314.
7. Choi BM, Kim BR. Upregulation of heme oxygenase-1 by brazilin via the phosphatidylinositol 3-kinase/Akt and ERK pathways and its protective effect against oxidative injury. *Eur J Pharmacol*. 2008;580:12–18.
8. Ndisang JF. Role of heme oxygenase in inflammation, insulin-signalling, diabetes and obesity. *Mediators Inflamm*. 2010; 2010:359732.
9. Kruger AL, Peterson SJ, Schwartzman ML, et al. Up-regulation of heme oxygenase provides vascular protection in an animal model of diabetes through its antioxidant and antiapoptotic effects. *J Pharmacol Exp Ther*. 2006;319:1144–1152.
10. Arai-Gaun S, Katai N, Kikuchi T, Kurokawa T, Ohta K, Yoshimura N. Heme oxygenase-1 induced in muller cells plays a protective role in retinal ischemia-reperfusion injury in rats. *Invest Ophthalmol Vis Sci*. 2004;45:4226–4232.
11. Sun MH, Pang JH, Chen SL, et al. Retinal protection from acute glaucoma-induced ischemia-reperfusion injury through pharmacologic induction of heme oxygenase-1. *Invest Ophthalmol Vis Sci*. 2010;51:4798–4808.
12. Sun MH, Pang JH, Chen SL, et al. Photoreceptor protection against light damage by AAV-mediated overexpression of heme oxygenase-1. *Invest Ophthalmol Vis Sci*. 2007;48:5699–5707.
13. Lin JH, Villalon P, Martasek P, Abraham NG. Regulation of heme oxygenase gene expression by cobalt in rat liver and kidney. *Eur J Biochem*. 1990;192:577–582.
14. Shibahara S, Müller RM, Taguchi H. Transcriptional control of rat heme oxygenase by heat shock. *J Biol Chem*. 1987;262: 12889–12892.
15. Desbuards N, Rochefort GY, Schlecht D, et al. Heme oxygenase-1 inducer hemin prevents vascular thrombosis. *Thromb Haemost*. 2007;98:614–620.
16. Morita K, Lee MS, Her S. Possible relation of hemin-induced HO-1 expression to the upregulation of VEGF and BDNF mRNA levels in rat C6 glioma cells. *J Mol Neurosci*. 2009;38: 31–40.
17. Zijlstra GS, Brandsma CA, Harpe MF, et al. Dry powder inhalation of hemin to induce heme oxygenase expression in the lung. *Eur J Pharm Biopharm*. 2007;67:667–675.
18. Nussler AK, Hao L, Knobeloch D, et al. Protective role of HO-1 for alcohol-dependent liver damage. *Dig Dis*. 2010;28:792–798.
19. Naughton P, Hoque M, Green CJ, Foresti R, Motterlini R. Interaction of heme with nitroxyl or nitric oxide amplifies heme oxygenase-1 induction: involvement of the transcription factor Nrf2. *Cell Mol Biol (Noisy-le-grand)*. 2002;48:885–894.
20. Kim J, Cha YN, Surh YJ. A protective role of nuclear factor-erythroid 2-related factor-2 (Nrf2) in inflammatory disorders. *Mutat Res*. 2010;690:12–23.
21. Calkins MJ, Johnson DA, Townsend JA, et al. The Nrf2/ARE pathway as a potential therapeutic target in neurodegenerative disease. *Antioxid Redox Signal*. 2009;11:497–508.
22. Gong P, Hu B, Cederbaum AI. Diallyl sulfide induces heme oxygenase-1 through MAPK pathway. *Arch Biochem Biophys*. 2004;432:252–260.
23. Balogun E, Hoque M, Gong P, et al. Curcumin activates the haem oxygenase-1 gene via regulation of Nrf2 and the antioxidant-responsive element. *Biochem J*. 2003;371:887–895.

24. Steinle JJ, Chin VC, Williams KP, Panjala SR. Beta-adrenergic receptor stimulation modulates iNOS protein levels through p38 and ERK1/2 signaling in human retinal endothelial cells. *Exp Eye Res*. 2008;87:30–34.
25. Ye X, Xu G, Chang Q, et al. ERK1/2 signaling pathways involved in VEGF release in diabetic rat retina. *Invest Ophthalmol Vis Sci*. 2010;51:5226–5233.
26. Livak KJ, Schmittgen TD. Analysis of relative gene expression data using real-time quantitative PCR and the $2^{-\Delta\Delta C}{}_T$ method. *Methods*. 2001;25:402–408.
27. Vidal-Sanz M, Villegas-Perez MP, Bray GM, Aguayo AJ. Persistent retrograde labeling of adult rat retinal ganglion cells with the carbocyanine dye DiI. *Exp Neurol*. 1988;102:92–101.
28. Ndisang JF, Jadhav A. Upregulating the heme oxygenase system suppresses left ventricular hypertrophy in adult spontaneously hypertensive rats for 3 months. *J Card Fail*. 2009;15:616–628.
29. Wang RQ, Nan YM, Wu WJ, et al. Induction of heme oxygenase-1 protects against nutritional fibrosing steatohepatitis in mice. *Lipids Health Dis*. 2011;10:31.
30. Natarajan R, Fisher BJ, Fowler AA III. Hypoxia inducible factor-1 modulates hemin-induced IL-8 secretion in microvascular endothelium. *Microvasc Res*. 2007;73:163–172.
31. Choi KM, Gibbons SJ, Nguyen TV, et al. Heme oxygenase-1 protects interstitial cells of Cajal from oxidative stress and reverses diabetic gastroparesis. *Gastroenterology*. 2008;135:2055–2064.
32. Fouad AA, Qureshi HA, Al-Sultan AI, Yacoubi MT, Ali AA. Protective effect of hemin against cadmium-induced testicular damage in rats. *Toxicology*. 2009;257:153–160.
33. Wang X, Ye XL, Liu R, et al. Antioxidant activities of oleanolic acid in vitro: possible role of Nrf2 and MAP kinases. *Chem Biol Interact*. 2010;184:328–337.
34. Bringmann A, Pannicke T, Grosche J, et al. Müller cells in the healthy and diseased retina. *Prog Retin Eye Res*. 2006;25:397–424.
35. de Melo Reis RA, Ventura AL, Schitine CS, de Mello MC, de Mello FG. Müller glia as an active compartment modulating nervous activity in the vertebrate retina: neurotransmitters and trophic factors. *Neurochem Res*. 2008;33:1466–1474.
36. Liu W, Xu GZ, Jiang CH, Da CD. Expression of macrophage colony-stimulating factor (M-CSF) and its receptor in streptozotocin-induced diabetic rats. *Curr Eye Res*. 2009;34:123–133.
37. Kowluru RA, Chan PS. Oxidative stress and diabetic retinopathy. *Exp Diabetes Res*. 2007;2007:43603.
38. Valdivia A, Pérez-Alvarez S, Aroca-Aguilar JD, Ikuta I, Jordán J. Superoxide dismutases: a physiopharmacological update. *J Physiol Biochem*. 2009;65:195–208.
39. Turan B. Role of antioxidants in redox regulation of diabetic cardiovascular complications. *Curr Pharm Biotechnol*. 2010;11:819–836.
40. Du Y, Miller CM, Kern TS. Hyperglycemia increases mitochondrial superoxide in retina and retinal cells. *Free Radic Biol Med*. 2003;35:1491–1499.
41. Craven PA, Melhem MF, Phillips SL, DeRubertis FR. Overexpression of Cu2+/Zn2+ superoxide dismutase protects against early diabetic glomerular injury in transgenic mice. *Diabetes*. 2001;50:2114–2125.
42. DeRubertis FR, Craven PA, Melhem MF, Salah EM. Attenuation of renal injury in db/db mice overexpressing superoxide dismutase: evidence for reduced superoxide-nitric oxide interaction. *Diabetes*. 2004;53:762–768.
43. Nyengaard JR, Ido Y, Kilo C, Williamson JR. Interactions between hyperglycemia and hypoxia: implications for diabetic retinopathy. *Diabetes*. 2004;53:2931–2938.
44. Arden GB, Sivaprasad S. Hypoxia and oxidative stress in the causation of diabetic retinopathy. *Curr Diabetes Rev*. 2011;7:291–304.
45. Goda N, Ryan HE, Khadivi B, McNulty W, Rickert RC, Johnson RS. Hypoxia-inducible factor 1alpha is essential for cell cycle arrest during hypoxia. *Mol Cell Biol*. 2003;23:359–369.
46. Ozaki H, Yu AY, Della N, et al. Hypoxia inducible factor-1alpha is increased in ischemic retina: temporal and spatial correlation with VEGF expression. *Invest Ophthalmol Vis Sci*. 1999;40:182–189.
47. Schmid T, Zhou J, Brüne B. HIF-1 and p53: communication of transcription factors under hypoxia. *J Cell Mol Med*. 2004;8:423–431.
48. Lin M, Chen Y, Jin J, et al. Ischaemia-induced retinal neovascularisation and diabetic retinopathy in mice with conditional knockout of hypoxia-inducible factor-1 in retinal Müller cells. *Diabetologia*. 2011;54:1554–1566.
49. Nakamura M, Kanamori A, Negi A. Diabetes mellitus as a risk factor for glaucomatous optic neuropathy. *Ophthalmologica*. 2005;219:1–10.
50. van Dijk HW, Verbraak FD, Kok PH, et al. Decreased retinal ganglion cell layer thickness in patients with type 1 diabetes. *Invest Ophthalmol Vis Sci*. 2010;51:3660–3665.
51. Panahian N, Yoshiura M, Maines MD. Overexpression of heme oxygenase-1 is neuroprotective in a model of permanent middle cerebral artery occlusion in transgenic mice. *J Neurochem*. 1999;72:1187–1203.
52. Adamis AP, Miller JW, Bernal MT, et al. Increased vascular endothelial growth factor levels in the vitreous of eyes with proliferative diabetic retinopathy. *Am J Ophthalmol*. 1994;118:445–450.
53. Aiello LP, Pierce EA, Foley ED, et al. Suppression of retinal neovascularization in vivo by inhibition of vascular endothelial growth factor (VEGF) using soluble VEGF-receptor chimeric proteins. *Proc Natl Acad Sci U S A*. 1995;92:10457–10461.
54. Ferrara N. Vascular endothelial growth factor. *Arterioscler Thromb Vasc Biol*. 2009;29:789–791.
55. Joussen AM, Poulaki V, Qin W, et al. Retinal vascular endothelial growth factor induces intercellular adhesion molecule-1 and endothelial nitric oxide synthase expression and initiates early diabetic retinal leukocyte adhesion in vivo. *Am J Pathol*. 2002;160:501–509.
56. Rangasamy S, McGuire PG, Das A. Diabetic retinopathy and inflammation: novel therapeutic targets. *Middle East Afr J Ophthalmol*. 2012;19:52–59.
57. Nguyen QD, Brown DM, Marcus DM, et al. RISE and RIDE Research Group. Ranibizumab for diabetic macular edema: results from 2 phase iii randomized trials: RISE and RIDE. *Ophthalmology*. 2012;119:789–801.
58. Yu DY, Cringle SJ, Su EN, Yu PK, Jerums G, Cooper ME. Pathogenesis and intervention strategies in diabetic retinopathy. *Clin Experiment Ophthalmol*. 2001;29:164–166.
59. International Expert Committee. International Expert Committee report on the role of the A1C assay in the diagnosis of diabetes. *Diabetes Care*. 2009;32:1327–1334.
60. American Diabetes Association. Diagnosis and classification of diabetes mellitus. *Diabetes Care Suppl 1*. 2010;33:S62–S69.